

Quark spin-orbit correlations in the proton

**M. Engelhardt,^{a,*} J. R. Green,^b N. Hasan,^c T. Izubuchi,^d C. Kallidonis,^e S. Krieg,^{f,g}
S. Liuti,^h S. Meinel,ⁱ J. Negele,^j A. Pochinsky,^j A. Rajan,^k G. Silvi^{c,l} and S. Syritsyn^m**

^a*Department of Physics, New Mexico State University, Las Cruces, NM 88003, USA*

^b*School of Mathematics and Hamilton Mathematics Institute, Trinity College Dublin, Dublin 2, Ireland*

^c*Bergische Universität Wuppertal, 42119 Wuppertal, Germany*

^d*Physics Department, Brookhaven National Laboratory, Upton, NY 11973, USA*

^e*Thomas Jefferson National Accelerator Facility, Newport News, VA 23606, USA*

^f*JARA & IAS, Jülich Supercomputing Centre, Forschungszentrum Jülich, 52425 Jülich, Germany*

^g*Helmholtz-Institut für Strahlen- und Kernphysik, Universität Bonn, 53115 Bonn, Germany*

^h*Department of Physics, University of Virginia, Charlottesville, VA 22904, USA*

ⁱ*Department of Physics, University of Arizona, Tucson, AZ 85721, USA*

^j*Center for Theoretical Physics, Massachusetts Institute of Technology, Cambridge, MA 02139, USA*

^k*Department of Physics, Old Dominion University, Norfolk, VA 23529, USA*

^l*Jülich Supercomputing Centre, Forschungszentrum Jülich, 52425 Jülich, Germany*

^m*Department of Physics and Astronomy, Stony Brook University, Stony Brook, NY 11794, USA*

E-mail: engel@nmsu.edu

Generalized transverse momentum-dependent parton distributions (GTMDs) provide a comprehensive framework for imaging the internal structure of the proton. In particular, by encoding the simultaneous distribution of quark transverse positions and momenta, they allow one to directly access longitudinal quark orbital angular momentum, and, moreover, to correlate it with the quark helicity. The relevant GTMD is evaluated through a lattice calculation of a proton matrix element of a quark bilocal operator (the separation in which is Fourier conjugate to the quark momentum) featuring a momentum transfer (which is Fourier conjugate to the quark position), as well as the Dirac structure appropriate for capturing the quark helicity. The weighting by quark transverse position requires a derivative with respect to momentum transfer, which is obtained in unbiased fashion using a direct derivative method. The lattice calculation is performed directly at the physical pion mass, using domain wall fermions to mitigate operator mixing effects. Both the Jaffe-Manohar as well as the Ji quark spin-orbit correlations are extracted, yielding evidence for a strong quark spin-orbit coupling in the proton.

The 38th International Symposium on Lattice Field Theory, LATTICE2021

26th-30th July, 2021

Zoom/Gather@Massachusetts Institute of Technology

*Speaker

1. Introduction

The dynamics of the angular momenta of the confined quarks in the proton constitute a central topic of hadron structure physics. Their description requires consideration of the full set of degrees of freedom available to quarks; orbital angular momentum (OAM) depends both on quark position and momentum, and the full quark angular momentum moreover includes the quark spin. A combined accounting for these characteristics is provided by (polarized) Wigner distributions that simultaneously encode position and momentum, or, equivalently, generalized transverse momentum-dependent parton distributions (GTMDs), which are related to the former by Fourier transformation: The quark impact parameter, i.e., transverse position, is Fourier conjugate to the transverse momentum transfer in the GTMD. The GTMD framework moreover provides control over the ambiguity in partitioning OAM among the quark and gluon degrees of freedom that is inherent in a gauge theory. Owing to gauge invariance, quark degrees of freedom cannot be considered in complete isolation, but must be accompanied by gluonic admixtures. The two most prominent schemes for defining these admixtures are the ones due to Ji [1] and to Jaffe and Manohar [2]. These schemes can be incorporated into the definition of GTMDs in well-defined fashion.

The GTMD framework has been employed to directly evaluate quark OAM in the proton in Lattice QCD calculations [3, 4], extending the scope of lattice considerations of OAM beyond the traditional avenue invoking Ji's sum rule [5], which is focused specifically on the Ji decomposition of OAM. A continuous, gauge-invariant interpolation between Ji and Jaffe-Manohar quark OAM was obtained, revealing that Jaffe-Manohar quark OAM is significantly enhanced in magnitude compared to Ji OAM, by approximately 30%. Upon incorporating methodological improvements of the treatment of the momentum transfer, using a direct derivative method [4], the result for Ji OAM was reconciled with the one obtained Ji's sum rule, validating the approach.

Quark OAM itself does not reference the quark spin, and is obtained from a GTMD in which the quarks are unpolarized. On the other hand, in view of the strong chromodynamic fields through which a quark in the proton propagates, the coupling of quark spin and OAM is expected to constitute an important dynamical determinant of the angular momentum budget in the proton. To obtain enhanced insight into the interplay between quark spin and OAM, it is useful to quantify quark spin-orbit correlations in the proton. These can be obtained in a manner that largely parallels the calculation of quark OAM; essentially, the counting of quarks has to be weighted by their spin, leading to the evaluation of a GTMD in which the quarks are polarized (in the nomenclature of [6], it is the GTMD G_{11} that encodes quark spin-orbit correlations). Here, a first lattice evaluation of quark spin-orbit correlations in the proton is presented, performed directly at the physical pion mass, employing a domain wall fermion ensemble furnished by the RBC/UKQCD collaboration.

2. Quark spin-orbit correlations

The longitudinal quark spin-orbit correlation $\langle 2L_3 S_3 \rangle$ in an unpolarized proton propagating in the 3-direction can be obtained from a GTMD matrix element [7],

$$\langle 2L_3 S_3 \rangle = \frac{1}{2P^+} \epsilon_{ij} \frac{\partial}{\partial z_{T,i}} \frac{\partial}{\partial \Delta_{T,j}} \frac{\langle p' | \bar{\psi}(-z/2) \gamma^+ \gamma^5 U[-z/2, z/2] \psi(z/2) | p \rangle}{S[U]} \Bigg|_{z^+ = z^- = 0, \Delta_T = 0, z_T \rightarrow 0} \quad (1)$$

which differs from the matrix element that determines longitudinal quark OAM, $\langle L_3 \rangle$, merely by the inclusion of the γ^5 structure weighting by helicity, and the fact that the proton state needs to be longitudinally polarized if one wishes to access OAM itself. A number of remarks are in order regarding eq. (1). The in- and outgoing proton momenta p, p' differ by a transverse momentum transfer Δ_T , i.e., $p = P - \Delta_T/2$, $p' = P + \Delta_T/2$, with the spatial component of P pointing in 3-direction. Given that Δ_T is Fourier conjugate to the quark impact parameter, b_T , taking the derivative with respect to Δ_T and evaluating it at $\Delta_T = 0$ corresponds to taking the average of b_T . Conversely, the operator separation z in the quark bilocal operator, which is also chosen to be purely transverse, $z \equiv z_T$, is Fourier conjugate to the transverse momentum k_T of the quark. Thus, taking the derivative with respect to z_T and evaluating it at $z_T = 0$ corresponds to taking the average of k_T . Here, caution must be exercised with respect to the limit $z_T \rightarrow 0$, which is associated with ultraviolet divergences. In (1), the Δ_T and z_T dependences are combined such as to yield the average $b_T \times k_T$, i.e., longitudinal OAM, correlated with the quark helicity through the $\gamma^+ \gamma^5$ Dirac structure. In view of the specification $z^+ = z^- = 0$, also the longitudinal quark momenta are integrated over.

In addition to this kinematic structure, eq. (1) depends on the choice of the Wilson line U , required by gauge invariance, that connects the quark operators. It is accompanied by a combined multiplicative soft and renormalization factor $\mathcal{S}[U]$ that compensates for the divergences associated with U . As in previous lattice TMD and GTMD studies [3, 4, 8–10], this factor will be canceled by forming an appropriate ratio of matrix elements in the further development below; as a result, it does not need to be specified further for present purposes. The choice of path for U is the feature that allows one to account for different definitions of quark OAM. As displayed in Fig. 1, staple-shaped paths $U \equiv U[-z/2, \eta v - z/2, \eta v + z/2, z/2]$ will be considered here, where the arguments of U denote positions that are joined by straight Wilson lines. The direction of the staple is given by the vector v , and its length by η .

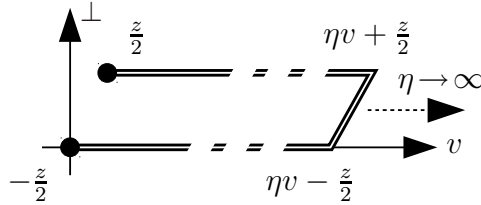


Figure 1: Gauge connection path in the matrix element (1).

The special case $\eta = 0$ corresponds to a straight Wilson line connecting the quark operators directly. This case yields the quark OAM according to the Ji decomposition of angular momentum [11]. On the other hand, a staple-shaped path extending to infinity, $\eta \rightarrow \pm\infty$, yields Jaffe-Manohar quark OAM [12]. In the context of standard TMDs, such a staple-shaped link is interpreted as incorporating final state interactions of a struck quark in a (semi-inclusive) deep inelastic scattering process as it is leaving the proton; the staple legs correspond to hard, eikonal propagators of the struck quarks. Accordingly, the difference between Jaffe-Manohar and Ji OAM has been interpreted in terms of the torque experienced by a struck quark [13]. The staple length η of course can be varied

(quasi-)continuously in a lattice calculation, and one thus obtains a gauge-invariant, continuous interpolation between the two limits.

Given the aforementioned physical role of the gauge link, a natural direction v for the staple would appear to be a lightlike vector, along which the struck quark propagates away from the hadron remnant. This choice, however, leads to rapidity divergences that call for regularization, with a standard scheme being to rotate v into the spacelike region [14, 15]. Then, (1) depends on an additional Collins-Soper type rapidity regulator that can be expressed in Lorentz-invariant fashion,

$$\hat{\zeta} = \frac{v \cdot P}{\sqrt{|v^2|} \sqrt{P^2}} \quad (2)$$

in terms of which the light-cone limit is approached for $\hat{\zeta} \rightarrow \infty$. As will be described below, this scheme is at the same time well-suited for casting the calculation of (1) as a lattice calculation.

It has already been noted above that, ultimately, a ratio of matrix elements will be constructed that serves to cancel the combined multiplicative soft and renormalization factor $\mathcal{S}[U]$. A quantity suitable for this purpose in the present context is the number of valence quarks

$$n = \frac{1}{2P^+} \left. \frac{\langle p' | \bar{\psi}(-z/2) \gamma^+ U[-z/2, z/2] \psi(z/2) | p \rangle}{\mathcal{S}[U]} \right|_{z^+ = z^- = 0, \Delta_T = 0, z_T \rightarrow 0} \quad (3)$$

which differs from (1) in that the weighting with $b_T \times k_T$ is omitted (thus, the matrix element simply counts quarks), and also the helicity weighting with γ^5 is missing. The latter choice is justified by the fact that domain wall fermions are used in the present calculation, respecting chiral symmetry, and therefore the vector and axial renormalization constants in the local limits of the operators coincide. For discretizations that break chiral symmetry, it would instead be appropriate to normalize specifically by the axial charge rather than the vector one. The factor $\mathcal{S}[U]$ is even in z_T and therefore cancels in the ratio $\langle 2L_3 S_3 \rangle / n$.

Preserving chiral symmetry in the fermion discretization moreover prevents the appearance of operator mixing effects [16–19] induced by the breaking of chiral symmetry. Such effects would invalidate the cancellation of renormalization factors through taking the ratio $\langle 2L_3 S_3 \rangle / n$, since they would generate additional additive terms in the numerator and denominator of the ratio.

At finite lattice spacing a , the derivative with respect to z_T in (1) is realized as a finite difference. The renormalized quantity therefore evaluated in practice is

$$\frac{\langle 2L_3 S_3 \rangle}{n} = \frac{1}{a} \epsilon_{ij} \left. \frac{\frac{\partial}{\partial \Delta_{T,j}} \left(\Phi^{[\gamma^+ \gamma^5]}(a\vec{e}_i) - \Phi^{[\gamma^+ \gamma^5]}(-a\vec{e}_i) \right)}{\Phi^{[\gamma^+]}(a\vec{e}_i) + \Phi^{[\gamma^+]}(-a\vec{e}_i)} \right|_{z^+ = z^- = 0, \Delta_T = 0} \quad (4)$$

where the transverse indices i and j are summed over, and $\Phi^{[\Gamma]}(z_T) = \langle p' | \bar{\psi}(-z/2) \Gamma U \psi(z/2) | p \rangle$. In the local limit $z_T \rightarrow 0$, (4) contains additional divergences, which, in view of the form of (4), are regularized by cutting off transverse momenta at the overall ultraviolet resolution of the calculation. This scheme a priori does not coincide with the standard \overline{MS} scheme, and a matching factor would be needed to connect to the latter. The results of the quark OAM calculation reported in [4] suggest that this matching factor, at least in the $\eta = 0$ limit, does not deviate significantly from unity within the statistical uncertainties typically achieved in these GTMD calculations.

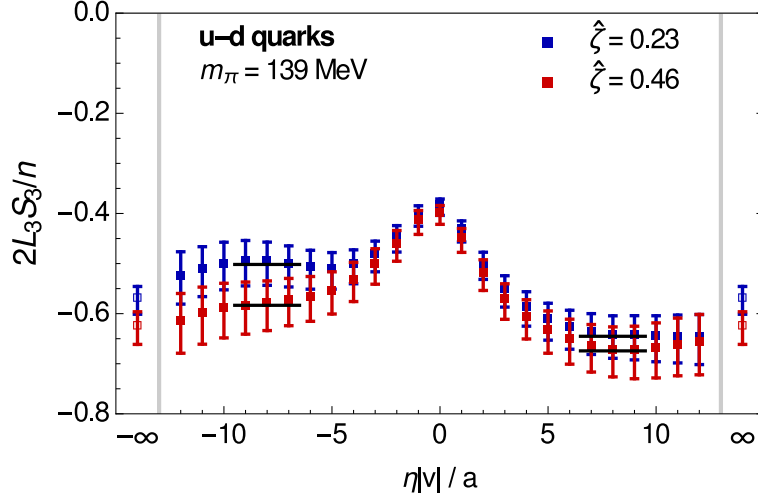


Figure 2: Quark spin-orbit correlation in the proton as a function of staple length η . The large- $|\eta|$ behavior is extracted from the plateau fits indicated by the black lines, where the values displayed for $\eta \rightarrow \pm\infty$ are obtained by averaging the plateaus obtained on the positive and negative η sides.

The derivative with respect to momentum transfer in (4), on the other hand, is realized employing an unbiased direct derivative method [20, 21], as laid out in detail for the GTMD calculations at hand in [4].

3. Lattice calculation and results

To cast the evaluation of (4) as a lattice calculation, it is necessary to boost (4) to a Lorentz frame in which the operator defining $\Phi^{[\Gamma]}(z_T)$ exists at a single time. This is the point for which a rapidity regulator scheme that renders the staple direction ν spacelike, as described above, is crucial; once all separations in the problem, i.e., z_T and $\eta\nu$, are spacelike, the requisite boost can be performed. After the boost, ν points into the (longitudinal) 3-direction, and both z_T and Δ_T lie in the transverse plane, orthogonal to each other.

The lattice calculation was performed using a domain wall fermion ensemble furnished by the RBC/UKQCD collaboration. The ensemble consisted of 130 lattices of extent $48^3 \times 96$ with spacing 0.114 fm and pion mass $m_\pi = 139$ MeV. An all-mode averaging scheme with 33280 low-accuracy and 520 exact samples for bias correction was employed. For this exploratory calculation, the fairly small source-sink separation $8a = 0.91$ fm was used in order to control statistical fluctuations. Calculations were performed for two proton momenta, $P_3 = 2\pi/(aL)$ and $P_3 = 4\pi/(aL)$ (where $L = 48$ is the spatial extent of the lattice). These correspond to the rapidity regulator values $\hat{\zeta} = 0.23$ and $\hat{\zeta} = 0.46$.

The numerical results are summarized in Fig. 2. Data for the isovector, $u-d$ quark combination are displayed, in which disconnected diagram contributions to the proton matrix elements cancel; such disconnected contributions were not evaluated in the present calculation. The quark spin-orbit correlation $\langle 2L_3 S_3 \rangle$ is shown as a function of the staple length η , interpolating between the $\eta = 0$ Ji limit and the $\eta \rightarrow \pm\infty$ Jaffe-Manohar limit, which is obtained by extrapolation. A marked

dependence on η is observed, which is even stronger than in OAM, $\langle L_3 \rangle$, considered by itself. In the latter case, the Jaffe-Manohar limit is enhanced in magnitude compared to the Ji limit by about 30% [4], whereas for the spin-orbit correlation, the enhancement is approximately 50%.

Comparing the results obtained for the two different values of the Collins-Soper type rapidity regulator $\hat{\zeta}$, no strong dependence can be discerned. Indeed, in the $\eta = 0$ limit, there can be no dependence on $\hat{\zeta}$, since in that limit there is no staple direction ν on which the results could depend. However, even in the large- $|\eta|$ Jaffe-Manohar limit, which in principle depends on $\hat{\zeta}$, no statistically significant variation is evident between the two surveyed values of $\hat{\zeta}$. This behavior was also seen for OAM itself [4], where merely the $\hat{\zeta} = 0$ data available in that calculation deviate significantly from the non-zero $\hat{\zeta}$ results. Seemingly, the large- $\hat{\zeta}$ limit is approached rather quickly in these observables.

The spin-orbit correlation is negative and its magnitude is considerable. As a point of reference, consider the uncorrelated product $2\langle L_3 \rangle \langle S_3 \rangle$ obtained in a longitudinally polarized proton. Of course, taking separate unpolarized averages over proton states, both factors in this product would be zero, whereas the spin-orbit correlation $\langle 2L_3 S_3 \rangle$ does not depend on whether the proton is longitudinally polarized or the unpolarized average is taken. The comparison is between, on the one hand, the indirect relative bias between quark OAM and quark spin induced by the proton being in any definite polarization state and, on the other hand, the direct correlation between quark OAM and quark spin. Taking recourse to the recent comprehensive study [5] of the Ji decomposition of proton spin at the physical pion mass, one has, for the two light quark flavors,

$$\langle L_3^u \rangle = -0.22(3), \quad 2\langle S_3^u \rangle = 0.86(2) \quad \Rightarrow \quad 2\langle L_3^u \rangle \langle S_3^u \rangle = -0.19(3) \quad (5)$$

$$\langle L_3^d \rangle = 0.26(2), \quad 2\langle S_3^d \rangle = -0.42(2) \quad \Rightarrow \quad 2\langle L_3^d \rangle \langle S_3^d \rangle = -0.11(1) \quad (6)$$

and, therefore, for the $u - d$ quark combination,

$$2\langle L_3^u \rangle \langle S_3^u \rangle - 2\langle L_3^d \rangle \langle S_3^d \rangle = -0.08(3) \quad (7)$$

amounting to only 1/5 of the direct correlation displayed in Fig. 2 at $\eta = 0$. Therefore, there is a strong direct dynamical coupling between quark OAM and spin, resulting in a correlation that far exceeds the simple bias for these quantities induced by the proton being in any definite polarization state. The quark OAM and spin are (anti-)aligned rather rigidly, while the angular momentum of the quark as a whole is, in comparison, less constrained in its orientation with respect to the angular momentum of the rest of the constituents of the proton. This is reminiscent of the jj coupling scheme in atomic physics, as opposed to the Russell-Saunders coupling scheme.

The result for the spin-orbit correlation obtained here is furthermore consistent with a phenomenological estimate obtained in [22] by connecting the spin-orbit correlation to moments of generalized parton distributions (GPDs), cf. also [23]. For the $u - d$ quark combination, the estimate obtained in [22] in the $\eta = 0$ Ji limit, $\langle 2L_3 S_3 \rangle \approx -0.37$, agrees well with the result exhibited in Fig. 2.

4. Summary

Generalized transverse momentum-dependent parton distributions (GTMDs) provide a comprehensive framework for parametrizing the internal structure of hadrons. The present work expands

the scope of Lattice QCD calculations of GTMD observables from the initial application to quark OAM in the proton [3, 4] to quark spin-orbit correlations, thus providing more detailed insight into the dynamical determinants of the proton's internal angular momentum structure. A strong, negative spin-orbit correlation is found, which moreover is significantly enhanced in magnitude, by about 50%, when one transitions from the Ji to the Jaffe-Manohar definition of OAM. By performing the lattice calculation using domain wall fermions directly at the physical pion mass, systematic uncertainties that would be engendered by breaking chiral symmetry in the fermion discretization, as well as ones associated with chiral extrapolation were eliminated; nonetheless, other systematic effects remain to be brought under control in future work, among them, e.g., excited state contaminations that may be significant for the fairly small source-sink separation employed in the present study.

Acknowledgments

Computing time granted by the John von Neumann Institute for Computing (NIC) and provided on the supercomputer JURECA [24] (Booster module) at Jülich Supercomputing Centre (JSC) is gratefully acknowledged, as are resources provided by the U.S. DOE Office of Science through the National Energy Research Scientific Computing Center (NERSC), a DOE Office of Science User Facility, under Contract No. DE-AC02-05CH11231. Calculations were performed employing the Qlua [25] software suite. S.M. is supported by the U.S. DOE, Office of Science, Office of High Energy Physics under Award Number DE-SC0009913. M.E., S.L., J.N. and A.P. are supported by the U.S. DOE, Office of Science, Office of Nuclear Physics through grants numbered DE-FG02-96ER40965, DE-SC0016286, DE-SC-0011090 and DE-FC02-06ER41444, respectively. S.S. is supported by the National Science Foundation under CAREER Award PHY-1847893. This work was furthermore supported by the U.S. DOE through the TMD Topical Collaboration.

References

- [1] X. Ji, Phys. Rev. Lett. **78**, 610 (1997).
- [2] R. Jaffe and A. Manohar, Nucl. Phys. **B337**, 509 (1990).
- [3] M. Engelhardt, Phys. Rev. **D 95**, 094505 (2017).
- [4] M. Engelhardt, J. R. Green, N. Hasan, S. Krieg, S. Meinel, J. Negele, A. Pochinsky and S. Syritsyn, Phys. Rev. **D 102**, 074505 (2020).
- [5] C. Alexandrou, S. Bacchio, M. Constantinou, J. Finkenrath, K. Hadjiyiannakou, K. Jansen, G. Koutsou, H. Panagopoulos and G. Spanoudes, Phys. Rev. **D 101**, 094513 (2020).
- [6] S. Meißner, A. Metz and M. Schlegel, JHEP **0908**, 056 (2009).
- [7] C. Lorcé and B. Pasquini, Phys. Rev. **D 84**, 014015 (2011).
- [8] B. Musch, P. Hägler, M. Engelhardt, J. Negele and A. Schäfer, Phys. Rev. **D 85**, 094510 (2012).

- [9] M. Engelhardt, P. Hägler, B. Musch, J. Negele and A. Schäfer, Phys. Rev. **D 93**, 054501 (2016).
- [10] B. Yoon, M. Engelhardt, R. Gupta, T. Bhattacharya, J. R. Green, B. Musch, J. Negele, A. Pochinsky, A. Schäfer, and S. Syritsyn, Phys. Rev. **D 96**, 094508 (2017).
- [11] X. Ji, X. Xiong and F. Yuan, Phys. Rev. Lett. **109**, 152005 (2012).
- [12] Y. Hatta, Phys. Lett. **B708**, 186 (2012).
- [13] M. Burkardt, Phys. Rev. **D 88**, 014014 (2013).
- [14] S. M. Aybat and T. Rogers, Phys. Rev. **D 83**, 114042 (2011).
- [15] J. C. Collins, *Foundations of Perturbative QCD*. Cambridge University Press, 2011.
- [16] M. Constantinou, H. Panagopoulos and G. Spanoudes, Phys. Rev. **D 99** (2019) 074508.
- [17] P. Shanahan, M. Wagman and Y. Zhao, Phys. Rev. **D 101** (2020) 074505.
- [18] J. Green, K. Jansen and F. Steffens, Phys. Rev. **D 101** (2020) 074509.
- [19] Y. Ji, J.-H. Zhang, S. Zhao and R. Zhu, Phys. Rev. **D 104** (2021) 094510.
- [20] G. M. de Divitiis, R. Petronzio and N. Tantalo, Phys. Lett. **B718**, 589 (2012).
- [21] N. Hasan, J. R. Green, S. Meinel, M. Engelhardt, S. Krieg, J. Negele, A. Pochinsky and S. Syritsyn, Phys. Rev. **D 97**, 034504 (2018).
- [22] C. Lorcé, Phys. Lett. **B735**, 344 (2014).
- [23] A. Rajan, M. Engelhardt and S. Liuti, Phys. Rev. **D 98**, 074022 (2018).
- [24] Jülich Supercomputing Centre, *JURECA: Modular supercomputer at Jülich Supercomputing Centre*. Journal of Large-Scale Research Facilities **4**, A132 (2018). <http://dx.doi.org/10.17815/jlsrf-4-121-1>
- [25] A. Pochinsky, *Qlua*. <https://usqcd.lns.mit.edu/qlua>.